Malaysian Journal of Chemistry, 2025, Vol. 27(4), 157-171

Thermal and Chemical Failure Analysis of Polymer-Based Waterproofing Membranes in High-Rise Residential Buildings

Nurul Fatahah Asyqin Zainal[1,2]*, Hairunnisa Ramli[1,2], Kuan You Wai[3], Yoga Sugama Salim[4] and Ester Goh Chung Chen[5]

[1]Centre of Foundation Studies, Universiti Teknologi MARA, Cawangan Selangor, Kampus Dengkil, 43800 Dengkil, Selangor, Malaysia

[2]RIG Sustainability Material Design and Manufacturing, Universiti Teknologi MARA, 40000 Shah Alam, Selangor, Malaysia

[3]PKN Building Solutions Sdn Bhd, 839 Lorong Permai 13A, Kampung Tasik Permai, 68000 Ampang, Selangor, Malaysia

[4]Matcor Technology & Services Pte. Ltd. (Cetim-Matcor), 3 Seletar Aerospace Link, 797550 Singapore

[5]Nippon Paint (M) Sdn Bhd, Lot 2A, Taman Perindustrian Subang Utama, Jalan SU 4, 40300 Shah Alam, Selangor, Malaysia

*Corresponding author (e-mail: nurulfa2916@uitm.edu.my)

The failure of waterproofing in residential buildings in Malaysia has become a serious problem that may result in structural damage and unsafe conditions. Thus, investigation into the factors that contribute to the failure of waterproofing is essential in reducing failure rates. This study was conducted to analyse failed waterproofing in comparison to successful waterproofing through evaluation of chemical and thermal properties using optical microscopy (OM), Fourier-transform infrared (FTIR) spectroscopy, thermogravimetric analysis (TGA), and differential scanning calorimetry (DSC). Two types of samples were studied, namely fibre-reinforced liquid-applied waterproofing and liquid-applied waterproofing. These waterproofing samples were extracted from two different locations (*i.e.*, at non-leaking and leaking areas). FTIR results revealed that both the leaking and non-leaking fibre-reinforced liquid-applied waterproofing samples exhibited similar absorption bands but had slightly different absorption intensities. The decomposition temperatures, T_d, were 397 °C (non-leaking sample) and 422 °C (leaking sample), while the glass transition temperatures, T_g, were 13 °C (non-leaking sample) and 9 °C (non-leaking sample). For the liquid-applied waterproofing samples, the FTIR absorbance spectrum of the leaking sample was different from that of the non-leaking sample. The waterproofing thickness values were 912 ± 40 μm (non-leaking sample) and 130 ± 40 μm (leaking sample), T_g values were 35 °C (non-leaking sample) and 52 °C (non-leaking sample), while the thermal decomposition of the leaking sample was significantly different from that of the non-leaking sample. Based on this data, inconsistencies in the quality of the waterproofing and improper installation techniques may have caused the failure. This study contributes physicochemical and thermal characterization techniques to the failure analysis of polymer-based waterproofing materials, offering guidance for waterproofing industry players towards enhancement of quality control processes and adherence to guidelines and standards.

Keywords: Waterproofing; failure analysis; thermogravimetric analysis; differential scanning calorimetry; Fourier-transform infrared

Received: May 2025; Accepted: June 2025

There are three main types of waterproofing, namely liquid waterproofing membranes, sheet-based waterproofing membranes, and cementitious waterproofing [1]. A liquid waterproofing membrane is applied through spraying, trowelling, rolling and brushing techniques, and allowed to set and form a membrane. It has the advantage of being seamless and easy to apply, which can minimize leakage through joints due to complicated detailing [1]. The sheet-based waterproofing membrane is made of either bitumen, thermoplastic polymers, thermosets, or rubber. It is usually applied by heat and often modified and bonded to a high-strength fabric, of polyester or fibreglass. This has better mechanical properties to protect against any stress caused by the normal structural expansion and contraction of a building. Lastly, cementitious waterproofing is a cement-based polymer coating that is often combined with acrylic latex as a binder to improve durability and cohesion, as well as tensile and flexural strength.

Tropical environments with high temperatures and intermittent rainfall [2] have made waterproofing crucial in buildings. Due to exposure to rain, UV

radiation, wind, and air pollution, buildings in tropical regions are prone to faster deterioration [3]. Water seepage is one of the main contributors to major defects and structural damage found in high-rise buildings [1, 4] and it accounts for 75 – 80 % of structural faults in buildings [5]. Water can get into a building structure through several mechanisms, namely natural gravitation, hydrostatic pressure, air currents, and surface tension [4]. It can enter a building through cracks, openings in the walls and roof, expansion joints, and porous surfaces [6]. Hence, exposed areas must be waterproofed to curb the seepage of water.

However, waterproofing frequently fails after several years of service, causing structural damage, water leakage, and unsafe conditions for the inhabitants of the building. Waterproofing failures may result from construction defects [1, 7, 8], material-related factors [9–11], and environmental factors [9–11]. Poor surface preparation, the presence of moisture, and improper detailing are common construction-related causes. Material-related failures include adhesion issues, reduced flexibility, and premature degradation due to poor formulation. Environmental factors include UV exposure, extreme temperatures, and humidity. While these factors often interact, this study focused on material-related failures, specifically the thermal and chemical properties of polymer-based waterproofing membranes. These material-related failures require analytical investigations to determine the underlying causes, which may arise from chemical processes such as hydrolysis, oxidation, UV exposure, or from improper formulation.

Despite the widespread use of polymer-based waterproofing membranes, studies that have systematically examined the material-related failures using a combination of thermal and chemical analyses [12], particularly in real-world building environments, are limited. Consequently, few solutions for failure prevention focusing on material-related failures have been put forward. Furthermore, the replacement or repair of failed waterproofing may be priced up to 5 – 10 % of the total cost of the project [13]. Hence, to avoid the additional expense, wastage of resources and time, as well as disastrous incidents, it is necessary to investigate the factors that lead to failure of waterproofing.

In this work, failure analysis was conducted on failed waterproofing membranes installed in high-rise residential buildings. The waterproofing membranes failed after eight years of service and resulted in water leakage on the ceilings and walls. After thorough inspection of the building, certain locations did not display signs of water leakage. Thus, failure analysis of the waterproofing was conducted by comparing the properties of the material at leaking and non-leaking locations. The analysis was conducted using optical microscopy (OM), Fourier transform infrared spectroscopy (FTIR), thermogravimetric analysis (TGA), and differential scanning calorimetry (DSC).

EXPERIMENTAL

Sample Collection

In 2016, two different types of waterproofing were installed in a high-rise residential building in Malaysia, covering the tennis court and rooftop. The first type of waterproofing, a fibre-reinforced liquid-applied waterproof membrane, was extracted from the tennis court. The second type of waterproofing, a liquid-applied waterproofing membrane, was extracted from the rooftop of the residential building. For each type of waterproofing, two samples were extracted at non-leaking and leaking locations (with visible signs of blistering and leakage), and these were labelled as non-leaking and leaking waterproofing samples. Figure 1 shows the samples extracted from the two locations. The size of each extracted sample was about 5 cm × 5 cm.

The waterproofing samples were carefully extracted from the concrete surface using a flat chisel and hammer, without disturbing the original morphology of the samples. Upon extraction, the samples were transported to the laboratory in sealed poly(ethylene) bags to prevent contamination. The samples were then cleaned using a soft-bristle brush to remove any loose debris, dust and concrete residue before being air-dried at 25 °C for 24 hours. All samples were stored in a desiccator to prevent further environmental degradation or moisture absorption. To maintain the integrity of the chemical and thermal properties of the samples, the storage duration prior to analysis did not exceed two weeks.

Characterization Methods

Optical Microscopy (OM)

The morphology of the samples was examined at 25 °C using an optical microscope (Soptop CX40M, Hong Kong, China) equipped with magnification lens of 10× and iSolution Lite ×64 software (Easley, USA). The thickness of the liquid-applied waterproofing membrane was determined by averaging measurements taken at nine distinct locations to ensure the accuracy of the results.

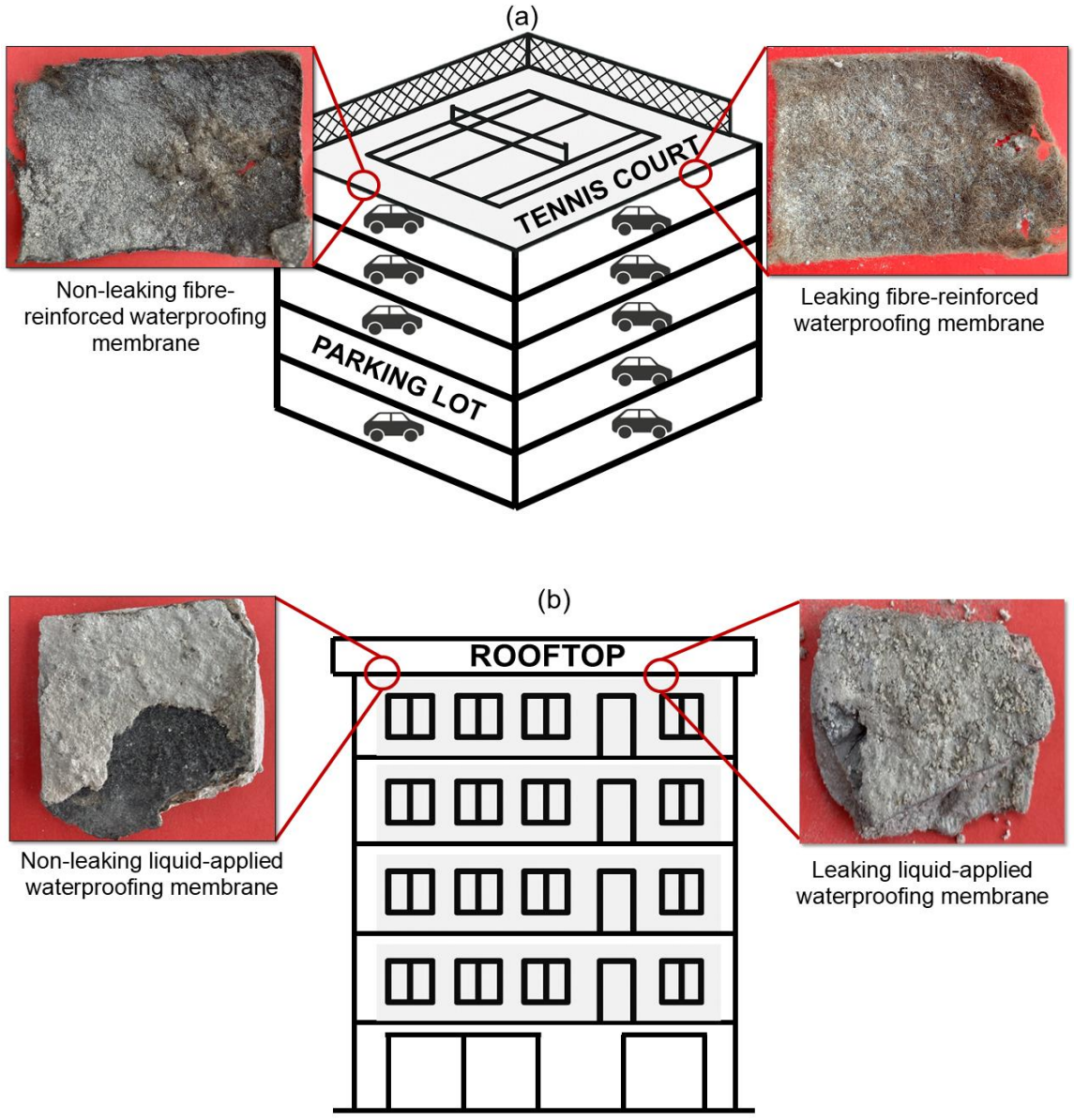

Figure 1. Illustration of samples extracted from two locations (a) non-leaking and leaking fibre-reinforced liquid-applied waterproofing membrane samples extracted from the tennis court and (b) non-leaking and leaking liquid-applied waterproofing membrane samples extracted from the rooftop.

The fibre distribution in the fibre-reinforced liquid-applied membranes was quantified using ImageJ software through image analysis of microstructural images. The image was first calibrated using the embedded scale bar, converted to 8-bit grayscale, and enhanced for contrast. A threshold was applied to segment the image into binary regions representing the fibres and the matrix, followed by conversion to a binary mask. Using the "Analyze Particles" function, the areas of fibres and matrix were measured, and estimation of fibre content was calculated using Equation 1 below:

$$\text{Fibre content (\%)} = \frac{\text{Fibre area}}{\text{Total image area}} \times 100 \qquad (1)$$

Fourier Transform Infrared (FTIR) Spectroscopy

FTIR spectra collection was carried out using the attenuated total reflectance (ATR) accessory with a diamond crystal window on Spectrum Two (Perkin Elmer, Waltham, Massachusetts). The spectra were recorded in absorbance mode in the range of 600 - 4000 cm^{-1} with 16 scans at a resolution of 2 cm^{-1} at room temperature (~ 25 °C). Each sample was analysed at three different spots to ensure that FTIR analysis was based on a representative region of the sample.

Quantitative analysis of the oxidation indices of the sulfoxide (S=O) group was carried out using

an integration method based on the area below the absorbance band around 1025 cm^{-1}. The aliphatic group (C−H bending) vibrations around 1453 and 1370 cm^{-1} were used as a reference due to the stability of these structures which are not affected by oxidation [14]. The baseline integration for each band was conducted using the tangential technique. The sulfoxide oxidation index was calculated using Equation 2 below:

$$\text{Sulfoxide index } (I_{S=O}) = \frac{A_{S=O}}{A_{\text{Reference}}} \quad (2)$$

where $A_{S=O}$ is the area of the band around 1025 cm^{-1} and $A_{\text{Reference}}$ is the area of the band around 1453 and 1370 cm^{-1}.

Thermogravimetric Analysis

The thermal stability of each sample was studied using a TGA Q500 (TA instrument, Delaware, USA). About 10 mg were used for a single measurement test and heated from 30 to 500 °C in a nitrogen atmosphere at a heating rate of 10 °C min^{-1}. The decomposition temperature, $T_{d\ (onset)}$ was estimated from the onset decomposition temperature determined from the thermogram. The thermal stability and mass change of the waterproofing membranes were evaluated using thermogravimetric analysis in accordance with ASTM E2550-11.

Differential Scanning Calorimetry (DSC)

The thermal properties of each sample was studied using a TA Q2000 (TA Instruments, Delaware, USA) equipped with RCS90 refrigerator cooling system (TA Instruments, Delaware, USA), with nitrogen gas purging throughout the experiment. Approximately 10 mg of sample was used for a single measurement test, cooled to −90 °C for 5 min and then heated to 180 °C at a rate of 10 °C min^{-1}. The glass transition temperature, T_g, change in heat capacity, ΔC_p, melting temperature, T_m and melting enthalpy, ΔH_m values were determined from the first heating cycle. T_g was taken at half of the ΔC_p value. ΔC_p was estimated from the glass transition of the onset and endset of the heat flow curve. The T_m value was taken at the melting peak maximum. ΔH_m was estimated from the area corresponding to the melting endotherm. The assignment of T_g and ΔH_m was conducted in accordance with ASTM E1356-08 and ASTM D3417-99, respectively.

RESULTS AND DISCUSSION

Analysis of the Fibre-reinforced Liquid-applied Waterproofing Membrane

Optical Microscopy

Morphological analysis of the fibre-reinforced liquid-applied waterproofing membranes, illustrated in Figure 2, revealed significant structural differences between the leaking and non-leaking samples. The leaking sample displayed a predominance of fibrous materials with a minimal presence of the waterproofing membrane matrix. In contrast, the non-leaking sample demonstrated a more balanced integration of fibres within the membrane material. This observation suggests that the leaking sample had an excessive amount of fibre reinforcement and an insufficient amount of waterproofing membrane. As a result, the fibres were inadequately bonded to the waterproofing matrix, leading to increased porosity in the membrane. The excessive fibre loadings may have led to poor dispersion of the fibres in the polymer matrix, resulting in agglomeration of the fibres [15], as can be observed in Figure 2(b). This may reduce the flexibility of the membrane, making it more prone to cracking under stress or substrate movement [16, 17]. An excessive amount of fibres may also disrupt the polymer matrix continuity, which reduces adhesion to the substrate and water impermeability [16, 17]. This finding aligns with the notion that a well-distributed and integrated matrix is critical to maintaining the impermeable properties of fibre-reinforced liquid-applied waterproofing membranes [18, 19].

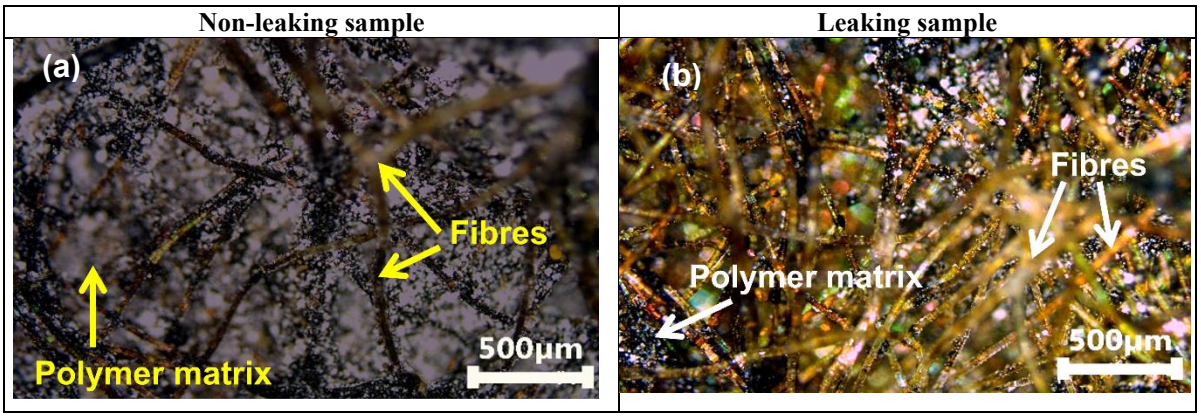

Figure 2. Micrographs of the top view of the (a) non-leaking and (b) leaking samples. The scale bar corresponds to 500 μm.

Table 1. The estimated fibre content of the fibre-reinforced liquid-applied membrane samples.

Sample	Fibre content (%)
Non-leaking membrane	48.1
Leaking membrane	75.2

Estimation of the fibre content in both the leaking and non-leaking membrane samples was performed using ImageJ software through image analysis, as described in the Methods section. The leaking membrane contained a significantly higher fibre content compared to the non-leaking membrane (see Table 1).

Chemical Structure Analysis

FTIR spectroscopy was employed to identify functional groups and quantify compounds in fibre-reinforced liquid-applied waterproofing membranes, a critical step in evaluating their performance and quality [20, 21]. Figure 3 presents the FTIR spectra of the non-leaking and leaking fibre-reinforced liquid-applied waterproofing membranes. Both samples showed similar absorption bands characteristic of bitumen-based materials, consistent with the literature [20–22]. These bands are indicative of a composition that includes bitumen, polymers, reinforcement material (e.g., polyester or fibreglass), and additives designed to create a durable and water-resistant membrane [23, 24]. The functional groups that were present in both samples are listed in Table 2.

As shown in Figure 3, the intensities of the absorbance bands were different for both samples. Absorption intensity is directly proportional to the concentration of the absorbing species in the sample [25]. The leaking sample showed reduced absorbance intensities at 2911 and 2851 cm^{-1}, signifying a lower concentration of aliphatic hydrocarbon compounds (key components in bitumen and polymers).

From previous reports, oxidative ageing of bitumen can be detected by the appearance of carbonyl (C=O) groups at 1690 cm^{-1} and sulfoxide (S=O) functional groups at 1030 cm^{-1} [26–28]. However, from Figure 3, there was no observable carbonyl group present in the leaking sample. Furthermore, a slightly higher intensity sulfoxide absorption band was observed in the leaking sample. The degree of oxidation indices of the sulfoxide group are listed in Table 3. This data suggests that there was minimal oxidative degradation of the sulfoxide group in the leaking sample.

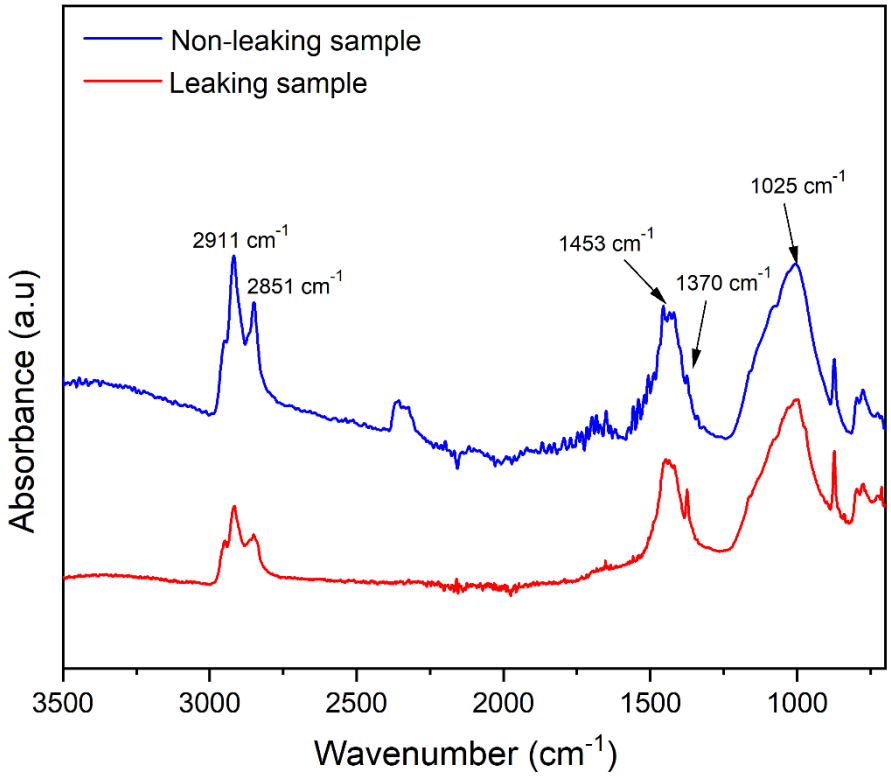

Figure 3. FTIR spectra of the fibre-reinforced liquid-applied waterproofing membrane samples.

Table 2. The functional groups present in both the non-leaking and leaking fibre-reinforced liquid-applied waterproofing membrane samples.

Wavenumber (cm^{-1})	Functional Groups and Band Characteristics	References
2911 and 2851	C−H stretching vibrations of aliphatic groups	[20, 22]
1453 and 1370	C−H bending vibrations of aliphatic rings	[20, 22]
1025	S=O stretching vibrations	[20, 22]

Table 3. The degree of oxidation indices of the sulfoxide group.

Sample	Degree of oxidation
Non-leaking	1.79
Leaking	1.82

Thermal Stability

The thermal stability and mass loss behaviour of the non-leaking and leaking samples are presented in Figure 4, and the findings are listed in Table 4. Both samples exhibited a single thermal degradation step, characteristic of fibre-reinforced liquid-applied waterproofing membranes [22]. Fibre reinforcement sheets are incorporated between polymer layers to enhance properties such as flexibility, durability, adhesion, and resistance to cracking in the waterproofing membranes [29].

The $T_{d\ (onset)}$ for the non-leaking sample was 397 °C, while for the leaking sample, it was 422 °C. The lower $T_{d\ (onset)}$ of the non-leaking sample reflects the effective interaction between the waterproofing material and the fibre reinforcement. T_d values at 50 % mass loss reported in previous studies were compared with the results of this work. Reported values range from 432 to 448 °C, which are relatively close to the T_d of the non-leaking sample (439 °C) [11, 22]. The small variation is likely due to differences in the formulation of the waterproofing membranes compared to those in the reported studies. Conversely, the higher $T_{d\ (onset)}$ of the leaking sample suggests the presence of excess fibre reinforcement, which increases thermal stability, as observed in similar polymer composite studies [30, 31]. This finding aligns with the highly fibrous morphology observed in the optical microscopy analysis.

At 500 °C, the mass retention of the non-leaking sample was significantly higher compared to that of the leaking sample. This difference indicates that the appropriate mixture of bitumen, polymer, and fibre reinforcement in the non-leaking sample synergistically enhances its thermal stability and slows down degradation [32, 33]. Additionally, the higher mass retention suggests a more stable and durable composition provided by the polymer component, which resists thermal degradation [11]. In contrast, the leaking sample's reduced mass retention is attributed to insufficient bitumen and polymer components, leading to more extensive degradation.

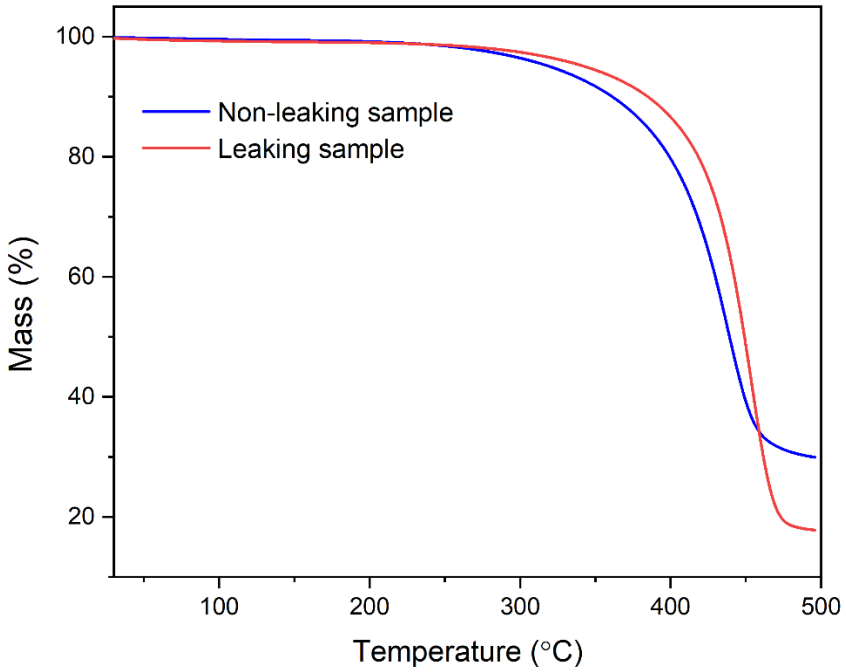

Figure 4. TGA thermograms of the fibre-reinforced liquid-applied waterproofing membrane samples.

Table 4. Thermal properties of the non-leaking and leaking fibre-reinforced liquid-applied waterproofing membrane samples.

Sample	Decomposition temperature, T_d (°C)	Mass retained (%)
Non-leaking sample	397	30
Leaking sample	422	18

Thermal Properties

As depicted in Figure 5, the T_g of the non-leaking sample was 13 °C, slightly higher than the leaking sample's T_g of 9 °C. The lower T_g for the leaking sample suggests that it transitions to a flexible, rubbery state at lower temperatures [34]. As a result, the leaking sample may exhibit reduced resistance to deformation or cracking, which could exacerbate leakage issues under mechanical or environmental stress [29].

The melting endotherms observed at 170 °C may be due to the presence of a fibre reinforcement component that is a semicrystalline polymer. In Figure 5, both samples displayed similar T_m values (~170 °C), confirming the presence of fibres in both samples. However, the leaking sample had a higher ΔH_m than the non-leaking sample. This indicates a higher energy requirement for the transition from solid to liquid phase. This is due to the greater proportion of crystalline regions, perhaps caused by the larger amount of fibres in the leaking sample [35].

The performance differences are thus largely attributed to variations in the amorphous regions and the amount of fibre reinforcement, as evidenced by the T_g and ΔH_m values [30,31]. The data extracted from the first heating cycle of the DSC analysis are summarized in Table 5.

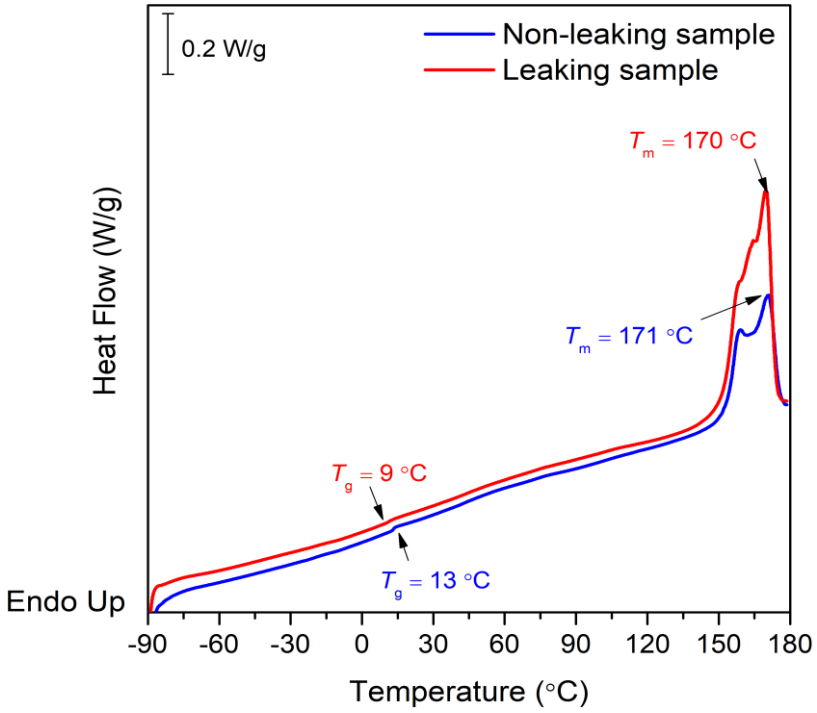

Figure 5. DSC traces of the fibre-reinforced liquid-applied waterproofing membrane samples.

Table 5. Thermal properties of the non-leaking and leaking fibre-reinforced liquid-applied waterproofing membrane samples.

Sample	Glass transition temperature, T_g (°C)	Melting temperature, T_m (°C)	Melting enthalpy, ΔH_m (J/g)
Non-leaking sample	13	171	36.4
Leaking sample	9	170	62.2

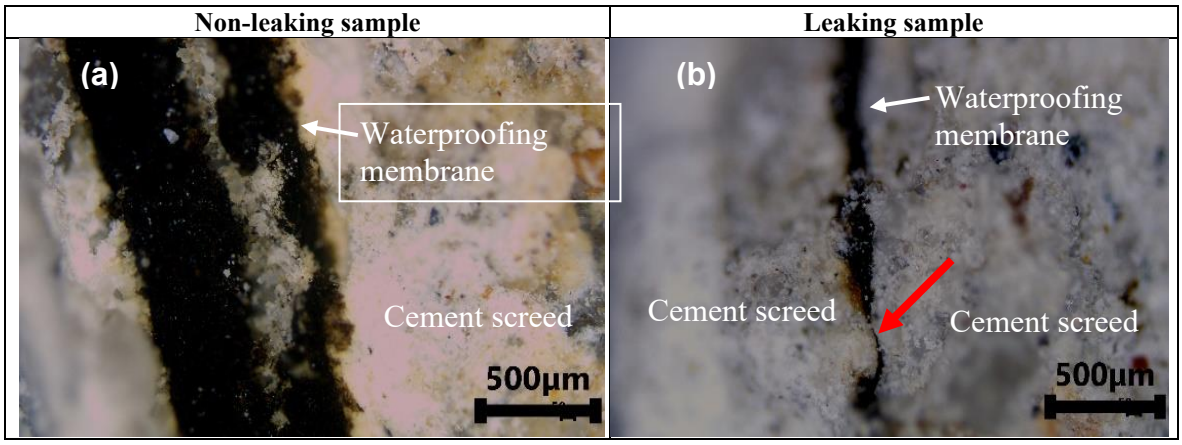

Figure 6. Micrographs of the cross-sections of the (a) non-leaking and (b) leaking samples. The scale bar corresponds to 500 μm.

Table 6. Average thickness values of the liquid-applied waterproofing membrane samples.

Sample	Average thickness (μm)
Non-leaking film	912 ± 40
Leaking film	130 ± 26

Analysis of the Liquid-applied Waterproofing Membrane

Optical Microscopy

The cross-section images of the non-leaking and leaking liquid-applied waterproofing membrane samples are shown in Figure 6 (a) and (b), respectively. The non-leaking sample appeared to be intact and uniform, whereas the leaking sample showed signs of discontinuity [red arrow in Figure 6 (b)]. The average thickness of the leaking sample was lesser than that of the non-leaking sample, as shown in Table 6. The observed reduced thickness and surface discontinuity indicates that the coating could potentially form more microcracks, allowing water to penetrate easily.

Chemical Structure Analysis

As presented in Figure 7, both liquid-applied waterproofing membranes displayed dissimilar FTIR spectra. The absence of absorbance bands at 2916 and 2845 cm^{-1}, which correspond to the symmetric and asymmetric stretching vibrations of C−H bonds in alkyl or methylene groups, indicates either degradation or removal of the hydrophobic chains. This is further supported by the reduction in the absorption intensity at 1423 cm^{-1} associated with C−H bending vibrations in alkanes. The reduced absorption intensity at 1020 cm^{-1} indicates changes in chemical additives or a loss of stabilizing agents that could affect the membrane's waterproofing efficacy. Additionally, a broad absorption band that appeared at 3330 cm^{-1} indicates water that was absorbed by the failed waterproofing in the leaking sample. This broad O−H band indicates possible hydrolytic degradation. Water ingress into the waterproofing membranes can accelerate degradation through hydrolysis of susceptible chemical bonds, leading to polymer chain scission [36]. Over time, this reaction may cause embrittlement, reduced flexibility and microcrack formation, which compromise waterproofing integrity [36, 37].

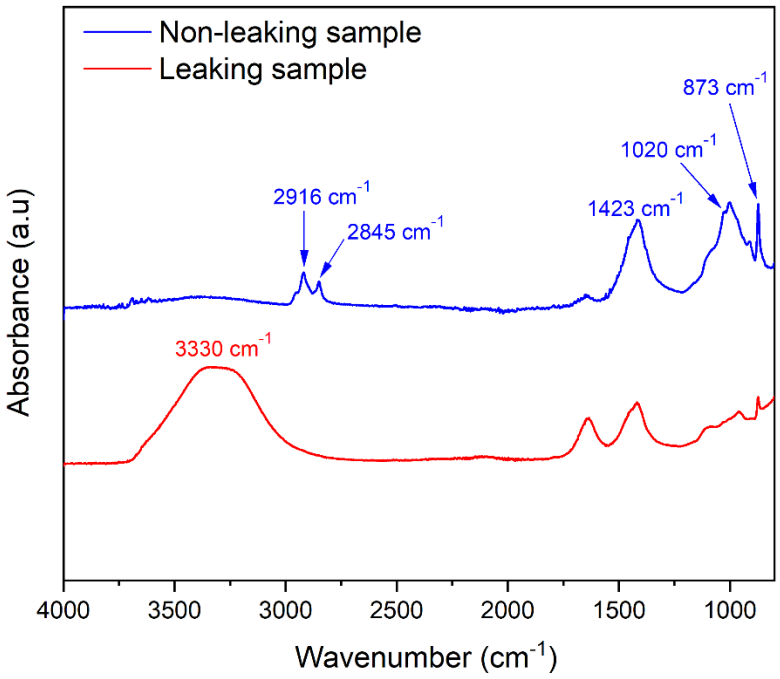

Figure 7. FTIR spectra of the liquid-applied waterproofing membrane samples.

Table 7. Functional groups in the non-leaking and leaking liquid-applied waterproofing membrane samples.

Non-leaking Sample		
Wavenumber (cm^{-1})	**Functional Groups and Band Characteristics**	**References**
2916 and 2845	C−H stretching vibrations of aliphatic groups	[1, 12]
1423	C−H bending vibrations of aliphatic rings	[1, 12]
1020	S=O stretching vibrations	[1, 12]
873	= C−H out of plane	[1, 13]
Leaking Sample		
Wavenumber (cm^{-1})	**Functional Groups and Band Characteristics**	**References**
3330	O−H stretching	
1423	C−H bending vibrations of aliphatic rings	[1, 12]
873	= C−H out of plane	[1, 13]

Thermal Stability

The TGA thermograms presented in Figure 8 reveal differing weight loss behaviour between the non-leaking and leaking liquid-applied waterproofing membrane samples, reflecting differences in their chemical composition and degradation mechanisms. For both samples, the initial weight loss occurred around 100 °C, which corresponds to the evaporation of moisture and the release of hydration water. This observation is consistent with the presence of water absorption bands identified in the FTIR spectrum at 3330 cm^{-1}. The membranes may absorb and retain some amount of water.

After the initial weight loss, the non-leaking membrane exhibited a single-stage weight loss beginning at approximately 250 °C and extending to 500 °C. Previous studies have also reported a single-stage weight loss in bitumen-polymer membranes occurring between approximately 250 °C and 500 °C, with a maximum degradation temperature observed around 400 – 450 °C [38–40]. This implies that the non-leaking membrane in this study contained enough bitumen and polymer for effective waterproofing. Moreover, the 26 % weight loss corresponds to the thermal decomposition of its waterproofing components, which include a mixture of bitumen, polymer, and various additives.

In contrast, the leaking sample showed a smaller, additional weight loss stage between 200 °C and 300 °C, followed by another minimal weight loss from 300 °C to 500 °C. The presence of an intermediate weight loss stage suggests the possible breakdown of poorly integrated or unstable components in the formulation. Furthermore, the absence of any major weight loss between 300 °C and 500 °C in the leaking sample indicates the absence or a minimal amount of a mixture of bitumen, polymer and additives.

Thermal Properties

Analysis of the liquid-applied waterproofing membrane samples by DSC revealed that both samples lacked a melting temperature (T_m), as shown in Figure 9. This absence confirms their amorphous nature [41–43]. Unlike crystalline materials that exhibit a sharp melting point [44–47], amorphous polymers transition more gradually, allowing them to maintain flexibility and resist crystallization [48], which are the key features for waterproofing applications.

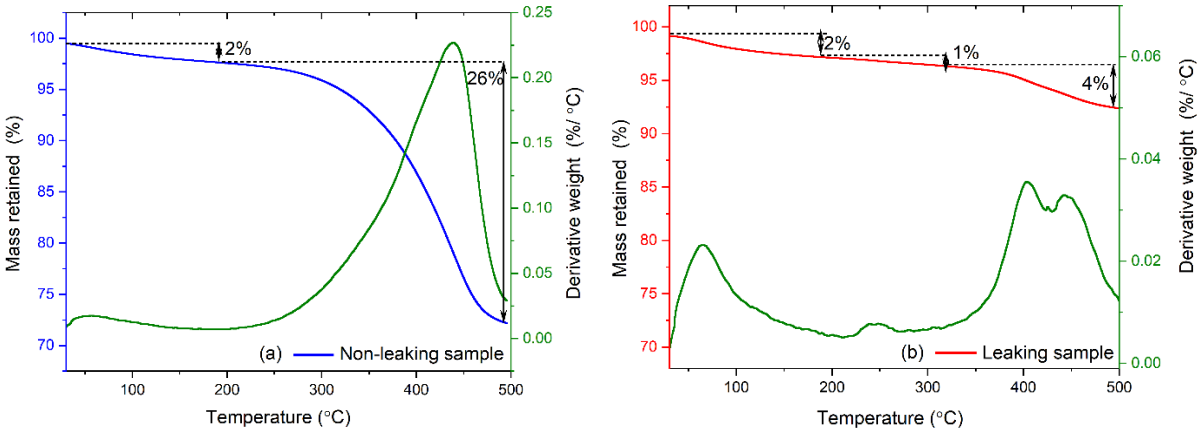

Figure 8. TGA thermograms of the (a) non-leaking and (b) leaking liquid-applied waterproofing membrane samples.

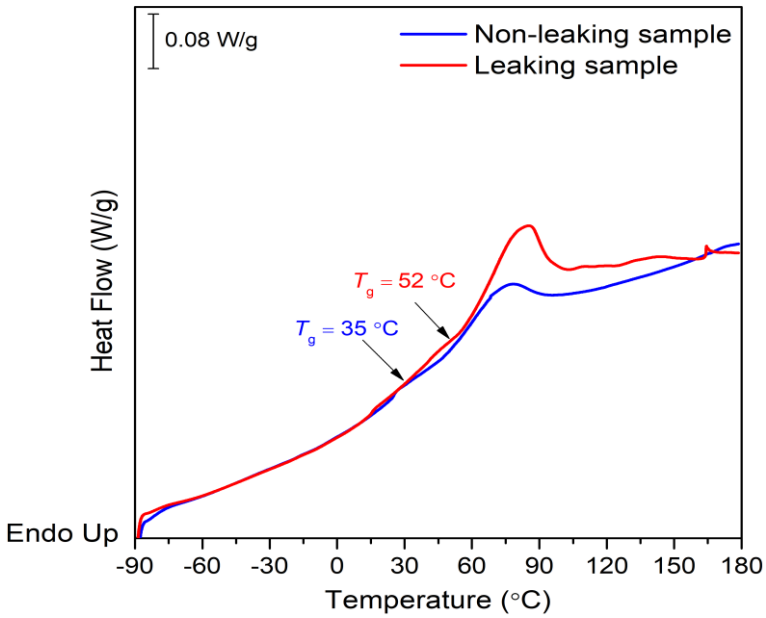

Figure 9. DSC traces of the liquid-applied waterproofing membrane samples.

Table 8. Thermal properties of the non-leaking and leaking liquid-applied waterproofing membrane samples.

Sample	Glass transition temperature, T_g (°C)	Change of Heat Capacity, ΔC_p (J/g °C)	Melting temperature, T_m (°C)	Melting enthalpy, ΔH_m (J/g)
Non-leaking sample	35	0.73	-	-
Leaking sample	52	1.07	-	-

A significant difference was observed in the T_g values of the two samples. The leaking sample had a T_g of 52 °C, notably higher than that of the non-leaking sample, which was 35 °C. This discrepancy indicates that the thermal properties of the leaking membrane had deviated from its intended composition, likely due to aging or material degradation. Furthermore, the leaking sample exhibited a larger ΔC_p value compared to the non-leaking sample. This suggests enhanced chain mobility or compositional changes in the material [34, 49]. The data obtained from the first heating cycle of the DSC analysis are summarized in Table 8 and reinforce the finding that the leaking membrane had undergone significant physical or chemical changes.

CONCLUSION

Analysis of both the fibre-reinforced liquid-applied waterproofing membrane and liquid-applied waterproofing membrane samples showed that the bitumen and polymer content was minimal in the leaking samples. This resulted in lower thermal stability, which reduced their ability to resist deformation or cracking. The reduced proportion of bitumen and polymer increases the amount of the fibre reinforcement, which does not contribute to water resistance as effectively as the bitumen-polymer blend.

In the case of the liquid-applied waterproofing membrane samples, the minimal amount or absence of bitumen and polymer further altered their thermal behaviour and caused them to exhibit different functional groups. The lower thickness of the leaking sample in comparison to the non-leaking one suggests issues with the application process, such as improper installation technique or formulation. These factors, combined with altered structural integrity, are major contributors to the gradual failure of the membranes.

There are several standards related to waterproofing materials. For instance, ASTM C836/C836M-18 and Singapore SS 374:1994(2023) describe the performance requirements and test methods for membranes used in waterproofing. ASTM D146-03 covers the sampling and examination of bitumen-saturated felts and fabrics for waterproofing, while ASTM C1305/C1305M outlines the procedure for determining the ability of a waterproofing compound to bridge a crack. Nevertheless, further improvements are recommended to reduce the risk of failure of waterproofing, as follows:

1. Continuous quality checks should be performed by manufacturers during material production to avoid inconsistencies and defects. Material certification should be conducted by an independent third-party to ensure the materials meet required specifications. Standards should be established to prevent performance variance in the waterproofing industry.

2. Mandatory training and certification from accredited institutions must be a prerequisite for site workers. These requirements should be included in tender and contract documents, stating clearly that only trained and certified workers are allowed to install waterproofing.

This study focused primarily on the thermal and chemical characteristics of failed waterproofing membranes, as mechanical performance tests such as tensile strength, crack bridging and peel adhesion were not conducted due to insufficient sample sizes. Moreover, the analysis was based on samples obtained from specific sites, which may not represent all types of waterproofing systems, materials or environmental conditions. For future studies, we recommend collecting a larger number of samples from different buildings and environments, performing mechanical testing, and applying accelerated aging methods, such as UV exposure, to better understand the performance of waterproofing membranes.

ACKNOWLEDGEMENTS

We gratefully acknowledge the Faculty of Applied Sciences, Universiti Teknologi MARA, for providing the laboratory space and facilities. We also wish to express our heartfelt gratitude and deepest respect to the late Professor Dr. Melissa Chan Chin Han for her invaluable guidance, inspiration, and role in initiating this failure analysis study. Though she is no longer with us, her influence continued to shape and inspire this work.

REFERENCES

1. Mydin, M. A. O., Nawi, M. N. M. & Munaaim, M. A. C. (2017) Assessment of waterproofing failures in concrete buildings and structures. *Malaysian Construction Research Journal*, **2**, 166–179.

2. Talib, R., Boyd, D., Hayhow, S., Ahmad, A. G. & Sulieman, M. (2015) Investigating Effective Waterproofing Materials in Preventing Roof Leaking; Initial Comparative Study: Malaysia, U.K. *Procedia Manufacturing,* **2**, 419–427.

3. Ahzahar, N., Karim, N. A., Hassan, S. H. & Eman, J. (2011) A study of contribution factors to building failures and defects in construction industry. *Procedia Engineering*, **20**, 249–255.

4. Kubal, M. T. (2008) Construction Waterproofing Handbook. *2nd ed.; McGraw Hill Education: New York*.

5. Elisabeth Heseltine & Rosen, J. (2009) WHO Guidelines for Indoor Air Quality: Dampness and Mould. *Heseltine, E., Rosen, J., Eds.; Copenhagen, Denmark*.

6. Senarathne, H. N. Y., Asmone, A. S. & Chew, M. Y. L. (2023) Developing a Waterproofing Decision-Making Model for High-Rise Building Projects in the Tropics. *Buildings*, **13**, 2328.

7. Mailvaganam, N. P. & Collins, P. G. (2004) Workmanship Factors Influencing Quality of Installed Parking Garage Waterproofing Membranes. *Journal of Performance of Constructed Facility*, **18**, 121–126.

8. Chew, M. Y. L. (2021) Design for maintainability of basements and wet areas. *Buildings*, **11**, 1–25.

9. Pedrosa, A. & Rio, M. Del. (2017) Comparative Scanning Electron Microscope Study of the Degradation of a Plasticized Polyvinyl Chloride Waterproofing Membrane in Different Conditions. *Materiales de Construcción*, **67**, 1–11.

10. Zagorodnikova, M. A., Yartsev, V. P. & Rupyshev, V. G. (2019) Strength and Durability of Roofing PVC Membranes in the Conditions of Climate Impacts. *Advanced Materials and Technology*, **2(14)**, 41–47.

11. Kaya, D., Topal, A., Gupta, J. & McNally, T. (2020) Aging effects on the composition and thermal properties of styrene-butadiene-styrene (SBS) modified bitumen. *Construction and Building Materials*, **235**, 117450.

12. Mendes, P., Lopes, J. G., de Brito, J. & Feiteira, J. (2014) Waterproofing of Concrete Foundations. *Journal of Performance of Constructed Facility*, **28**, 242–249.

13. Bauer, E., Vasconcelos, P. H. C. & Granato, J. E. (2010) Sistemas de impermeabilização e isolamento térmico. Materiais de construção civil e princípios de ciência e engenharia de materiais. *2nd ed.; IBRACON: São Paulo*.

14. Lamontagne, J., Dumas, P., Mouillet, V. & Kister, J. (2001) Comparison by Fourier transform infrared (FTIR) spectroscopy of different ageing techniques: Application to road bitumens. *Fuel*, **80**, 483–488.

15. Faludi, G., Hári, J., Renner, K., Móczó, J. & Pukánszky, B. (2013) Fiber association and network formation in PLA/lignocellulosic fiber composites. *Composite Science and Technology*, **77**, 67–73.

16. Webo, W., Masu, L. M. & Nziu, P. K. (2022) Formulation of nanocellulosic fibres and particle fillers, and their mono and hybrid reinforced polymer composites. *Materials Research Express*, **9(3)**, 035404.

17. George, G., Dev, A. P., Asok, N. N., Anoop, M. S. & Anandhan, S. (2021) Dispersion analysis of nanofillers and its relationship to the properties of the nanocomposites. *Material Today: Proceeding*, **47**, 5104–5109.

18. Subramaniyan, P. S., Imam, M. A. & Prabhakar, P. (2021) Fiber packing and morphology driven moisture diffusion mechanics in reinforced composites. *Composites Part B Engineering*, **226**, 109259.

19. Mohammed, M., Rahman, R., Mohammed, A. M., Adam, T., Betar, B. O., Osman, A. F. & Dahham, O. S. (2022) Surface treatment to improve water repellence and compatibility of natural fiber with polymer matrix: Recent advancement. *Polymer Testing*, **115**, 107707.

20. Ratajczak, M. (2017) Spectral Analysis of Polymer Modified Bitumen Used in Waterproofing. *Journal of Civil Engineering Environment and Architure*, **64**, 113–123.

21. Zofka, A., Maliszewska, D., Maliszewski, M. & Boratyński, J. (2015) Application of FTIR ATR method to examine the polymer content in the modified bitumen and to assess susceptibility of bitumen to ageing. *Roads and Bridges - Drogi i Mosty*, **14(3)**, 163–174.

22. Chen, M., Geng, J., Chen, H., Niu, Y. & He, L. (2022) Micro-characterization of bitumens under the coupling action of moisture and oxygen. *Journal of Building and Engineering,* **53**, 104589.

23. Llinas, P. & Breul, B. (2023) Bituminous Geomembrane (BGM) in hot climates for hydraulic construction. In *E3S Web of Conference*, **368**, 02011.

24. Buckner, C. A., Lafrenie, R. M., Dénommée, J. A., Caswell, J. M., Want, D. A., Gan, G. G., Leong, Y. C., Bee, P. C., Chin, E., Teh, A. K. H., et al. (2016) Intech Open, **11**, 13.

25. Jiang, J., Zhang, S., Longhurst, P., Yang, W. & Zheng, S. (2021) Molecular structure characterization of bituminous coal in Northern China via XRD, Raman and FTIR spectroscopy. *Spectrochimica Acta - Part A Molecular Biomolecular Spectroscopy*, **255**, 119724.

26. Sá Da Costa, M., Farcas, F., Santos, L., Eusébio, M. I. & Diogo, A. C. (2010) Chemical and thermal characterization of road bitumen ageing. *Material Science Forum*, **636**, 273–279.

27. He, Y., Zhang, T., Mao, S., Zeng, S., Wu, L. & Yu, J. (2024) Investigation of Antiaging Performance and Service Life of OMMT/SBS Modified Bitumen Waterproof Membranes. *Journal of Material and Civil Engineering*, **36(4)**, 1–12.

28. Hofko, B., Porot, L., Falchetto Cannone, A., Poulikakos, L., Huber, L., Lu, X., Mollenhauer, K. & Grothe, H. (2018) FTIR spectral analysis of bituminous binders: reproducibility and impact of ageing temperature. *Materials and Structures*, **51**, 1-16.

29. Kim, J. Il, Gong, M. H., Song, J. Y., Oh, S. K. & Kim, B. (2020) A study of waterproof reinforcement layers for the post-cracking behavior of fiber reinforced concrete. *Applied Sciences*, **10**, 1–15.

30. Huang, H., Pang, H., Huang, J., Zhao, H. & Liao, B. (2020) Synthesis and characterization of ground glass fiber reinforced polyurethane-based polymer concrete as a cementitious runway repair material. *Construction and Building Materials*, **242**, 117221.

31. Asyraf, M. R. M., Nurazzi, N. M., Norrrahim, M. N. F., Hazrati, K. Z., Ghani, A., Sabaruddin, F. A., Lee, S. H., Shazleen, S. S. & Razman, M. R. (2023) Thermal properties of oil palm lignocellulosic fibre reinforced polymer composites: a comprehensive review on thermogravimetry analysis. *Cellulose*, **30(5)**, 2753-2790.

32. Chen, X., Li, M., Yu, M. & Li, Y. (2024) Preparation and performance study of waterproof and breathable layer of alginate/aramid-based fabrics and flame-retardant multilayer combination. *Designed Monomers and Polymers*, **27(1)**, 1–14.

33. Abd-Elnaiem, A. M., Hussein, S. I., Ali, N. A., Hakamy, A. & Mebed, A. M. (2022) Ameliorating the Mechanical Parameters, Thermal Stability, and Wettability of Acrylic Polymer by Cement Filling for High-Efficiency Waterproofing. *Polymers*, **14(21)**, 4671.

34. Menczel, J. D. & Prime, R. B. (2009) Thermal Analysis of Polymers: Fundamentals and Applications. *John Wiley & Sons, Inc, New Jersey*.

35. Dole, M. & Wunderlich, B. (1959) Melting points and heats of fusion of polymers and copolymers. *Die Makromolekulare Chemie*, **34**, 29–49.

36. Croll, S. G. (2022) Stress and embrittlement in organic coatings during general weathering exposure: A review. *Progress in Organic Coatings*, **172**, 107085.

37. Zieliński, K., Babiak, M., Ratajczak, M. & Kosno, J. (2017) Impact of Chemical and Physical Modification on Thermoplastic Characteristics of Bitumen. *Procedia Engineering*, **172**, 1297–1304.

38. Wei, K., Ma, B. & Duan, S. Y. (2019) Preparation and Properties of Bitumen-Modified Polyurethane Solid–Solid Phase Change Materials. *Journal of Material and Civil Engineering*, **31(8)**, 04019139.

39. Izquierdo, M. A., Navarro, F. J., Martínez-Boza, F. J. & Gallegos, C. (2012) Bituminous polyurethane foams for building applications: Influence of bitumen hardness. *Construction and Building Materials*, **30**, 706–713.

40. Chen, Y., Hu, J., Wu, X., Duan, S., Wang, H. & Ma, T. (2024) Synthesis and Evaluation of Polyurethane as Waterproof Adhesion Layer for Steel Bridge Deck. *Polymers*, **16(22)**, 3140.

41. Schindler, A., Doedt, M., Gezgin, Ş., Menzel, J. & Schmölzer, S. (2017) Identification of polymers by means of DSC, TG, STA and computer-assisted database search. *Journal of Thermal Analysis and Calorimetry*, **129(2)**, 833–842.

42. Ramli, H., Chan, C. H., Ali, A. M. M. (2017) Thermal Properties and Intermolecular Interaction

of Binary Polymer Blends of Poly(ethylene oxide) and Poly(n-butyl methacrylate). In *Applied Chemistry and Chemical Engineering*, **4**, 77-91.

43. Abdul Halim, S. I., Chan, C. H. & Sim, L. H. (2016) Thermal properties and intermolecular interaction of blends of poly(ethylene oxide) and poly(methyl acrylate). *Macromolecular Symposia*, **365**, 95–103.

44. Gray, A. P. (1970) Polymer crystallinity determinations by DSC. *Thermochimica Acta*, **1(6)**, 563–579.

45. Hoffman, J. D. & Weeks, J. (1962) Melting Process and the Equilibrium Melting Temperature of Polychlorotrifluoroethylene. *Journal of Research of the National Bureau of Standards. Section A, Physics and Chemistry*, **66(1)**, 13.

46. Wang, X. Y. & Salovey, R. (1987) Melting of ultrahigh molecular weight polyethylene. *Journal of Applied Polymer Science*, **34**, 593–599.

47. Kong, Y. & Hay, J. N. (2002) The measurement of the crystallinity of polymers by DSC. *Polymer*, **43(14)**, 3873–3878.

48. Li, Y., Huang, P., Gao, Y., Sheng, J., Li, W. & Wang, F. (2024) Effect of waterproofing materials on resistivity and pore properties of concrete under insolation and rain. *Construction Building and Materials*, **425**, 136108.

49. dos Santos, W. N., de Sousa, J. A. & Gregorio, R. (2013) Thermal conductivity behaviour of polymers around glass transition and crystalline melting temperatures. *Polymer Testing*, **32(5)**, 987–994.